Safety and Efficacy of Pembrolizumab in Combination with Acalabrutinib in Advanced Head and Neck Squamous Cell Carcinoma: Phase 2 Proof-of-Concept Study

Matthew H. Taylor[1], Courtney B. Betts[2], Lauren Maloney[1,2], Eric Nadler[3], Alain Algazi[4], Michael J. Guarino[5], John Nemunaitis[6], Antonio Jimeno[7], Priti Patel[8], Veerendra Munugalavadla[8], Lin Tao[8], Douglas Adkins[9], Jerome H. Goldschmidt Jr[10], Ezra E.W. Cohen[11], and Lisa M. Coussens[2]

ABSTRACT

Purpose: Programmed cell death-1 (PD-1) receptor inhibitors have shown efficacy in head and neck squamous cell carcinoma (HNSCC), but treatment failure or secondary resistance occurs in most patients. In preclinical murine carcinoma models, inhibition of Bruton's tyrosine kinase (BTK) induces myeloid cell reprogramming that subsequently bolsters CD8^{+} T cell responses, resulting in enhanced antitumor activity. This phase 2, multicenter, open-label, randomized study evaluated pembrolizumab (anti–PD-1 monoclonal antibody) plus acalabrutinib (BTK inhibitor) in recurrent or metastatic HNSCC.

Patients and Methods: Patients received pembrolizumab 200 mg intravenously every 3 weeks, alone or in combination with acalabrutinib 100 mg orally twice daily. Safety and overall response rate (ORR) were co-primary objectives. The secondary objectives were progression-free survival (PFS) and overall survival.

Results: Seventy-six patients were evaluated (pembrolizumab, $n = 39$; pembrolizumab + acalabrutinib, $n = 37$). Higher frequencies of grade 3–4 treatment-emergent adverse events (AE; 65% vs. 39%) and serious AEs (68% vs. 31%) were observed with

combination therapy versus monotherapy. ORR was 18% with monotherapy versus 14% with combination therapy. Median PFS was 2.7 [95% confidence interval (CI), 1.4–6.8] months in the combination arm and 1.7 (95% CI, 1.4–4.0) months in the monotherapy arm. The study was terminated due to lack of clinical benefit with combination treatment. To assess how tumor immune contexture was affected by therapy in patients with pre- and post-treatment biopsies, spatial proteomic analyses were conducted that revealed a trend toward increased CD45^{+} leukocyte infiltration of tumors from baseline at day 43 with pembrolizumab (monotherapy, $n = 5$; combination, $n = 2$), which appeared to be higher in combination-treated patients; however, definitive conclusions could not be drawn due to limited sample size.

Conclusions: Despite lack of clinical efficacy, immune subset analyses suggest that there are additive effects of this combination; however, the associated toxicity limits the feasibility of combination treatment with pembrolizumab and acalabrutinib in patients with recurrent or metastatic HNSCC.

Introduction

Head and neck squamous cell carcinoma (HNSCC) is the seventh most common cancer in the world, with approximately 600,000 new cases diagnosed each year (1). At diagnosis, approximately 60% of patients with HNSCC present with locoregionally advanced disease associated with poor survival, and a majority develops local and/or regional recurrences; 20% to 30% develop distant metastasis (2, 3). Patients with HNSCC harboring human papillomavirus (HPV) within

their neoplastic epithelial cells tend to exhibit better prognoses than patients with HPV[−] tumors (4). Patients with HPV[−] disease typically exhibit T cell–suppressive tumor-immune microenvironments (TiME) and have significantly greater risk of disease recurrence and shorter survival rates than patients with HPV[+] tumors (4–6). The programmed cell death-1 (PD-1) immune checkpoint inhibitor pembrolizumab is approved in the United States in combination with platinum and 5-fluorouracil chemotherapy for patients with metastatic or unresectable HNSCC and as monotherapy for patients with

---

[1]Division of Hematology and Oncology, Knight Cancer Institute, Oregon Health and Science University, Portland, Oregon. [2]Department of Cell, Developmental, and Cancer Biology, Knight Cancer Institute, Oregon Health and Science University, Portland, Oregon. [3]Baylor University Medical Center, Dallas, Texas. [4]University of California San Francisco, San Francisco, California. [5]Helen F. Graham Cancer Center and Research Institute, Newark, Delaware. [6]University of Toledo College of Medicine and Life Sciences, and ProMedica Health System, Toledo, Ohio. [7]University of Colorado Cancer Center, Denver, Colorado. [8]AstraZeneca, South San Francisco, California. [9]Washington University School of Medicine, St. Louis, Missouri. [10]Blue Ridge Cancer Care, Blacksburg, Virginia. [11]University of California San Diego, Moores Cancer Center, La Jolla, California.

Current address for M.H. Taylor: Earle A. Chiles Research Institute, Portland, OR; and current address for J. Nemunaitis: Gradalis, Inc., Carrollton, TX.

Corresponding Authors: Lisa M. Coussens, Knight Cancer Institute, Oregon Health and Science University, 2720 S Moody Avenue, Portland, OR 97201. Phone: 503-494-7811; Fax: 503-494-4253; E-mail: coussenl@ohsu.edu; and Matthew H. Taylor, Earle A. Chiles Research Institute 4805 NE Glisan Street, 2N140, Portland, Oregon 97213. Phone: 503-215-6614; Fax: 503-215-6841; E-mail: Matthew.Taylor@providence.org

Translational Relevance

Anti–PD-1 resistance and poor survival in patients with head and neck squamous cell carcinoma (HNSCC) are attributed to the T cell–suppressing tumor-immune microenvironment, which is characterized by presence of antitumor response-suppressing immune cells. Bruton's tyrosine kinase (BTK) inhibition has been reported to regulate tumor growth suppression by effecting tumor-associated inflammation. Clinical data from a phase 2 study investigating the combination of the BTK inhibitor acalabrutinib and PD-1 inhibitor pembrolizumab compared with pembrolizumab alone were assessed for safety and efficacy in patients with advanced HNSCC. Combination therapy was associated with a higher rate of both treatment-emergent and serious adverse events, with no efficacy benefit seen. Despite the lack of clinical efficacy, tumor immune contexture data revealed that combination-treated patients had greater CD45$^+$ leukocyte tumor infiltration. Additional research with larger sample sizes would be needed to assess the impact of this therapy on the tumor microenvironment in patients with HNSCC.

metastatic or unresectable HNSCC tumors expressing programmed death-ligand 1 (PD-L1; combined positive score ≥1; ref. 7). However, approximately 60% of patients with relapsed or metastatic HNSCC show primary (i.e., nonresponsive neoplastic cells) or adaptive resistance (i.e., tumor cell–extrinsic mechanisms, such as those regulated by the immune system, which recognize the neoplastic cells and adapt to the immune attack) to PD-1–targeted therapies (8). Thus, there is a substantial unmet clinical need for improved treatment strategies for patients with advanced HNSCC.

Several characteristics of the HNSCC TiME contribute to immune suppression and resistance to PD-1 inhibitors, including significant densities of regulatory T cells (Treg), tumor-associated macrophages, and a paucity of CD8$^+$ T cells (8). Bruton's tyrosine kinase (BTK) is a non-receptor protein tyrosine kinase expressed in cells of multiple hematopoietic lineages that plays a critical role in myeloid cell maturation, trafficking, and function (9). In both transgenic and orthotopic insulinoma (10) and pancreatic ductal adenocarcinoma (PDAC; refs. 11, 12) murine models, BTK was identified as a key regulator of tumor-associated inflammation, where BTK inhibition resulted in increased presence of tumor-associated CD8$^+$ T cells correlating with suppressed tumor growth (11). More recently, data from a murine, cisplatin-resistant, oral squamous cell carcinoma xenograft model showed that inhibition of BTK, with and without chemotherapy, suppressed tumor growth and re-sensitized tumors to cisplatin (13). In addition, BTK knockdown led to downregulation of the immune checkpoint receptor TIM-3, which is selectively expressed on CD4$^+$ and CD8$^+$ T cells (13). Acalabrutinib is a next-generation, potent, highly selective, small-molecule covalent inhibitor of BTK that is approved in adults with previously treated mantle cell lymphoma and in patients with chronic lymphocytic leukemia or small lymphocytic lymphoma (14).

We hypothesized that reprogramming the tumor myeloid compartment through BTK inhibition in combination with PD-1 inhibition might facilitate improved CD8$^+$ T cell tumor infiltration and antitumor activity. The objectives of the current study were to assess the safety and antitumor activity of acalabrutinib in combination with pembrolizumab versus pembrolizumab monotherapy in patients with advanced HNSCC, and to evaluate local tumor immune response via spatial proteomic profiling of immune contexture.

Patients and Methods

Study participants

Eligible patients were men and women ≥18 years of age with an Eastern Cooperative Oncology Group (ECOG) performance status of 0 or 1; confirmed, radiologically measurable (per RECIST 1.1), recurrent, metastatic or unresectable HNSCC of the oral cavity, oropharynx, hypopharynx, or larynx; and progression during or after platinum-based chemotherapy or recurrence within 6 months after platinum-based neoadjuvant or adjuvant therapy. Patients with a prior malignancy other than HNSCC, except for adequately treated basal cell or squamous cell skin cancer, *in situ* cervical cancer, or other cancer from which the subject had been disease free for ≥2 years or that would not limit survival to <2 years, were not eligible for this study. Patients also were excluded from the study if they had received prior therapy with any inhibitor of BTK, protein kinase B (Akt), JAK, mTOR, PI3K, or Syk, or prior therapy with an anti–PD-1, anti–PD-L1, anti–PD-L2, anti-CD137, or anti–CTLA-4 antibody (including ipilimumab, nivolumab, pembrolizumab, MPDL3280A, or any other antibody or drug specifically targeting T cell co-stimulation or immune checkpoint pathways). Patients with any of the following conditions were also ineligible for participation in this trial: Central nervous system metastases and/or carcinomatous meningitis; a life-threatening illness or any medical condition (including psychiatric conditions) that, in the investigator's opinion, could compromise the patient's safety; or significant cardiovascular disease such as uncontrolled or symptomatic arrhythmias, congestive heart failure, or myocardial infarction within 6 months of starting study drug.

Study design and treatment

This was a phase 2, multicenter, open-label, randomized study evaluating pembrolizumab monotherapy versus the combination of pembrolizumab plus acalabrutinib in patients with recurrent, metastatic, or unresectable treatment-refractory HNSCC. Eligible patients were randomized 1:1 to receive pembrolizumab 200 mg intravenously every 3 weeks or pembrolizumab 200 mg intravenously every 3 weeks for a maximum of 24 months plus acalabrutinib 100 mg orally (capsules) twice daily. Acalabrutinib capsules were not permitted to be opened or dissolved, crushed, or administered as a suspension. Compliance with acalabrutinib dosing was assessed on the basis of review of the patient's completed drug diary and tabulation of the remaining capsules at each study visit. Patients with disease progression while receiving pembrolizumab monotherapy were allowed to cross over to combination treatment with acalabrutinib and pembrolizumab. Patients who crossed over to combination therapy were permitted to continue treatment until disease progression or the development of dose-limiting toxicity (DLT; defined in Supplementary Methods). Dose reductions of acalabrutinib were permitted (level 1, 100 mg once daily; level 2, 50 mg twice daily) for DLTs. Only dose interruption or discontinuation of pembrolizumab was permitted. Patients with disease progression while receiving combination therapy discontinued study treatment.

Tumor biopsies were collected from patients participating in the optional tumor biopsy portion of the study at baseline and after 43 days of treatment. Baseline tumor tissues were obtained from either an archived sample or the most recent pre-treatment biopsy; primary or metastatic site tumor tissue was permitted. The study was conducted according to the principles of the Declaration of Helsinki and the International Conference on Harmonization Guidelines for Good Clinical Practice, and the study protocol was reviewed and approved

by the independent ethics committee/institutional review board at the study centers. All participants provided their written informed consent before entering the study. The study was registered on ClinicalTrials.gov (identifier NCT02454179).

Study endpoints and assessments

The primary objectives of the study were to characterize the safety profile of pembrolizumab plus acalabrutinib combination therapy and to determine the overall response rates (ORR; defined as complete and partial responses) for pembrolizumab monotherapy and pembrolizumab plus acalabrutinib. The secondary study objectives were to assess progression-free survival (PFS) and overall survival (OS) in each treatment arm. Exploratory objectives were to assess the pharmacokinetics (PK) of acalabrutinib alone and in combination with pembrolizumab and to examine the effects of pembrolizumab plus acalabrutinib on tumor-infiltrating T cells and myeloid cells.

Safety profile evaluations included assessments of adverse events (AE), abnormalities of laboratory tests, and DLTs. The severity of AEs and laboratory abnormalities were graded using the Common Terminology Criteria for Adverse Events, version 4.03. Standard criteria were used to define serious AEs (SAE; Supplementary Methods). Events of clinical interest (ECI) for pembrolizumab plus acalabrutinib were selected for further analysis based on preclinical findings, emerging data from clinical studies, and findings from post-marketing studies for pembrolizumab. Relative dose intensity was defined as the ratio of the actual cumulative dose to the planned cumulative dose through the drug exposure period. A pre-planned interim safety analysis was conducted to assess DLTs after 6 patients were successfully randomized to the combination treatment arm of the study and treated for at least 4 weeks. Enrollment was paused for the interim safety analysis, which occurred on November 24, 2015. No DLTs were reported, and the safety committee approved enrollment into the expansion phase of the study based on these results.

Efficacy endpoints included ORR, disease control rate (DCR; defined as a response of stable disease or better), duration of response (DOR), PFS, and OS, and were based on assessments of tumor response according to RECIST version 1.1. Radiologic tumor assessments by CT were completed at baseline; weeks 7, 13, and 19; and then every 12 weeks (or more frequently at the investigator's discretion). Patients who discontinued study drug were followed for tumor assessment until disease progression or initiation of any other anticancer therapies, whichever came first.

Plasma samples for acalabrutinib PK assessments were collected pre-dose, and at 0.5, 1, 2, and 4 hours post-dose on day 1 and weeks 1, 3, and 7 from the first 6 patients in the combination arm per interim safety analysis. A pre-dose sample was also taken on day 2 of week 1. For all other subjects enrolled in the combination arm, blood samples were taken pre-dose and 1 hour post-dose on week 3. These samples were analyzed for acalabrutinib using a validated LC/MS-MS method, with an analytic range for acalabrutinib of 1.00 to 1,000 ng/mL. The following PK parameters were calculated for acalabrutinib: AUC from the time of dosing to the time of the last measurable concentration ($AUC_{0\text{-last}}$), observed maximum concentration (C_{max}), and time at which C_{max} occurred (T_{max}).

PD-L1 status was assessed centrally at Q^2 Solutions using a Dako 22C3 antibody (Agilent Technologies).

Tumor-infiltrating T cell, B cell, and myeloid cell subsets were evaluated using a sequential multiplex immunohistochemical (mIHC) platform and validated lineage-selective antibodies as previously described (15, 16). HNSCC tissue staining and image processing were completed as previously described, including staining for p16 and determination of HPV status (15), with new data visualization used for the current study. For staining of clinical trial specimens, slides were prepared following standard IHC methodology, then specimens were incubated with primary antibody, detected by a secondary antibody-labeled polymer-based peroxidase, visualized by chromogenic reaction with an alcohol-soluble peroxidase substrate, and digitally scanned. Specimens were then washed in ethanol and heat-stripped of antibodies to allow for iterative cycles of staining on each biopsy. After sequential IHC staining, the scanned images were processed by a digital image workflow to produce coregistered images (MATLAB, The MathWorks, Inc.), followed by nuclear segmentation and extraction of chromogenic signal (FIJI, FIJI Is Just ImageJ), and single-cell quantification (CellProfiler, Broad Institute). The computational pipeline culminated with immune cell classification via hierarchical gating (FCS Express, De Novo software) as previously described (15) and shown in Supplementary Fig. S1. Myeloid and lymphoid lineage cells were phenotyped using three 11+ antibody panels encompassing 26 epitopes distinctive of myeloid and lymphoid cell subsets and a functional biomarker panel (Supplementary Table S1). The myeloid biomarker panel identified myelomonocytic cells by CD68 (as no results were recorded for CSF1R), encompassing both monocytes and macrophages, immature (DC-LAMP$^-$) versus mature (DC-LAMP$^+$) dendritic cells (DC), CD66b$^+$ granulocytes (Gr), including neutrophils and eosinophils, and tryptase$^+$ mast cells. The lymphoid biomarker panel identified CD8$^+$ T cells; T-helper (Th)0, Th1, Th2, and Th17 cells; Tregs; B cells; and natural killer cells. Cell type abundance was depicted as cell density (the number of cells counted divided by square millimeters of tissue), proportions of cell populations (i.e., %CD45$^+$ of total nucleated cells), or ratios of cell types (counts of cell type X/counts of cell type Y from same size/region of tissue).

Statistical analyses

The study sample size was determined by a Z-test for normal approximation of binomial distribution, based on one-sided $\alpha = 0.10$, 80% power, with projected response rates of 40% in the pembrolizumab plus acalabrutinib combination arm and 18% in the pembrolizumab monotherapy arm. The final planned sample size was 37 patients in each arm. Power Analysis and Sample Size Software version 11 were used to conduct the sample size calculation.

Safety and efficacy analyses were conducted in all patients who received at least one dose of study drug (either pembrolizumab or acalabrutinib). Patients originally randomized to the pembrolizumab monotherapy arm who crossed over to receive pembrolizumab plus acalabrutinib combination therapy were included in the pembrolizumab monotherapy group for all analyses unless otherwise indicated.

Database lock occurred on October 4, 2018. Descriptive statistics were used to summarize safety and efficacy variables. For PK assessments, a noncompartmental PK approach was used to analyze individual plasma acalabrutinib concentration–time data (using Phoenix WinNonlin version 7.0). For mIHC assessments, differences in immune cell abundance in stacked bar graphs (cell density) were assessed using multiple t tests with Bonferroni–Dunn multiple comparison correction. For comparison of baseline with on-treatment values, a paired non-parametric t test (Wilcoxon matched-pairs signed rank test) was used with alpha = 0.05.

Results

Immune contexture and BTK$^+$ expression in human HNSCC

Preclinical murine models of pancreatic adenocarcinoma identified that BTK is significantly expressed by myeloid cells in the

TiME and is a significant regulator of myeloid cell functionality and myeloid-mediated T cell suppression (10–12). To investigate immune contexture and cell type–specific expression of BTK in leukocyte subsets infiltrating human HNSCC tumors in general and as stratified by HPV status, we quantitatively assessed overall density differences in $CD45^+$ leukocytes, $CD68^+$ myeloid cells, $CD3^+$ T cells, and $CD20^+$ B cells in 38 primary HNSCC tumors using a tissue microarray of HNSCC surgical resections (ref. 15; **Fig. 1A** and **B**). These analyses revealed that the $CD45^+$ cell infiltration into HNSCC tumors was largely driven by $CD3^+$ T cells (**Fig. 1B**), and when stratified by HPV status using p16 positivity as a molecular correlate, HPV^+ HNSCC contained significantly increased density of $CD3^+$ T cells with no significant difference in density of $CD20^+$ B cells or $CD68^+$ myeloid cells based on HPV status (**Fig. 1A** and **B**). To reveal cell type–specific expression of BTK in these major leukocyte lineages, we evaluated BTK in $CD20^+$ B cells; $CD68^+$ myelomonocytic cells; $CD163^+$ myelomonocytic cells (CD163 is a high-affinity scavenger receptor correlating with regulatory functionality); and tryptase-positive mast cells in a tissue microarray containing both HPV^+ and HPV^- HNSCC (15). These analyses revealed a paucity of BTK^+ B cells, whereas myeloid subsets expressing BTK were readily identified in HNSCC tumors independent of HPV status (**Fig. 1C** and **D**). On the basis of these findings and those previously reported from the murine preclinical modeling (10–12), we hypothesized a functional role for myeloid cell BTK in mediating T cell suppression in HNSCC.

Study population

To investigate this hypothesis in the clinical setting, 78 patients were enrolled between May 26, 2015 and July 5, 2018 at 18 study centers and randomized to receive pembrolizumab monotherapy ($n = 39$) or pembrolizumab plus acalabrutinib combination therapy ($n = 39$; Supplementary Fig. S2). Of the 39 patients originally randomized to the pembrolizumab monotherapy arm, 14 crossed over to receive pembrolizumab plus acalabrutinib combination therapy. Two patients randomized to the pembrolizumab plus acalabrutinib arm did not receive study medication.

Baseline demographics and disease characteristics were similar between treatment groups (**Table 1**). Overall, the median age was 60.5 years (range, 38–97 years), 76% of patients had an ECOG performance status of 1, and 61% had disease stage IVC. The median number of prior systemic regimens was 2 (range, 1–7), with 42% of patients having received ≥3 prior regimens. The median time on study was 9.2 months (range, 0.7–32.7 months) in the pembrolizumab monotherapy arm and 6.4 months (range, 0.8–34.1 months) in the pembrolizumab plus acalabrutinib combination therapy arm. Among patients who crossed over to combination therapy, the median time on study was 12.0 months (range, 2.4–32.7 months). All patients ultimately discontinued the study (Supplementary Fig. S2). The primary reason for study discontinuation was death, which was reported in 49 (63%) patients. An additional 18 (23%) patients discontinued from the study due to sponsor termination of the study, 5 (6%) patients voluntarily withdrew from the study, and 6 (8%) discontinued for other reasons [hospice care ($n = 4$), patient withdrew consent ($n = 1$), patient unable to swallow pills ($n = 1$)]. Among all patients who received pembrolizumab ($n = 76$) or acalabrutinib ($n = 51$) as part of any treatment arm during the study, the most common reasons for discontinuation of pembrolizumab or acalabrutinib treatment were progressive disease [$n = 44$ (57.9%) and $n = 29$ (56.9%), respectively] and AEs [$n = 10$ (13.2%) and $n = 11$ (21.6%), respectively].

Safety

The median duration of pembrolizumab treatment was 3.5 months (range, 0.03–24.18 months) and the median relative dose intensity for pembrolizumab was 100% (range, 50%–100%). For the 14 patients who crossed over from pembrolizumab monotherapy to combination therapy with pembrolizumab and acalabrutinib, the median duration of pembrolizumab monotherapy treatment was 2.8 months (range, 1.38–15.90 months). The median duration of acalabrutinib treatment was 3.0 months (range, 0.23–24.18 months) and the median relative dose intensity for acalabrutinib was 98% (range, 10%–100%).

All treated patients experienced ≥1 treatment-emergent AE of any grade (**Table 2**). Grade 3–4 AEs, serious AEs, and AEs leading to treatment discontinuation were less frequent in the pembrolizumab monotherapy arm versus the pembrolizumab plus acalabrutinib arm (**Table 2**). The most frequent any-grade AEs experienced by ≥25% of patients were fatigue ($n = 20$; 51%) in the monotherapy arm and fatigue ($n = 14$; 38%), dyspnea ($n = 13$, 35%), anemia ($n = 12$, 32%), decreased appetite ($n = 11$, 30%), diarrhea ($n = 11$, 30%), dehydration ($n = 10$, 27%), and pyrexia ($n = 10$; 27%) in the combination treatment arm. The most common serious AEs occurring in at least 3 patients were tumor hemorrhage ($n = 3$; 8%) in the monotherapy arm and dyspnea ($n = 4$; 11%), acute kidney injury ($n = 3$; 8%), and pneumonia ($n = 3$; 8%) in the combination treatment arm. The only AE that led to treatment discontinuation in more than 1 patient was dysphagia ($n = 3$, all in the combination treatment arm; 8%).

Any-grade AEs related to pembrolizumab as assessed by the investigators occurred in 59% of patients in the monotherapy arm (grade 3–4, 8%) and in 30% of patients in the combination arm (grade 3–4, 16%). AEs related to acalabrutinib as assessed by the investigators occurred in 32% of patients (grade 3–4, 8%), and AEs related to both pembrolizumab and acalabrutinib occurred in 51% of patients (grade 3–4, 16%; **Table 2**). The grade 3–4 pembrolizumab treatment-related AEs were rash, pruritus, hyponatremia, hyperglycemia, syncope, and dysphagia (3% each) in the monotherapy arm, and anemia, autoimmune hepatitis, diarrhea, dysphagia, epiglottitis, lichen planus, nausea, and vomiting (3% each) in the combination treatment arm. Grade 3–4 acalabrutinib-related AEs were fatigue (5%) and decreased appetite (3%). Grade 3–4 AEs related to both pembrolizumab and acalabrutinib treatment were anemia, increased alanine aminotransferase, and pneumonia (all reported in the same patient, 3%), and neutropenia, pain in extremity, rash, stomatitis, and weight decreased (3% each).

The most frequent any-grade ECIs occurring in ≥10% of patients in either the pembrolizumab monotherapy or pembrolizumab plus acalabrutinib arm were infections (39% and 76%, respectively), immune-mediated endocrinopathies-thyroid disorders (10% and 5%), anemia (8% and 32%), and transaminase elevations (0% and 11%). The most common any-grade infection events occurring in ≥10% of patients in either the pembrolizumab monotherapy or pembrolizumab plus acalabrutinib arms were pneumonia (13% and 22%, respectively), upper respiratory tract infection (5% and 16%), and cellulitis (3% and 11%). The only grade ≥3 ECI reported in ≥10% of patients in either treatment arm was infection, which was reported in 3 patients (8%) in the pembrolizumab monotherapy arm and 8 patients (22%) in the pembrolizumab plus acalabrutinib arm.

A total of 26 deaths were reported in the pembrolizumab monotherapy arm (10 receiving crossover treatment at time of death), and 23 deaths were reported in the pembrolizumab plus acalabrutinib combination arm. The most common cause of death was disease progression, reported in 22 (56%) patients in the monotherapy arm (including 8 patients receiving crossover treatment) and 18 (49%) patients in the combination arm. A total of 6 (8%) patients died due to AEs, including
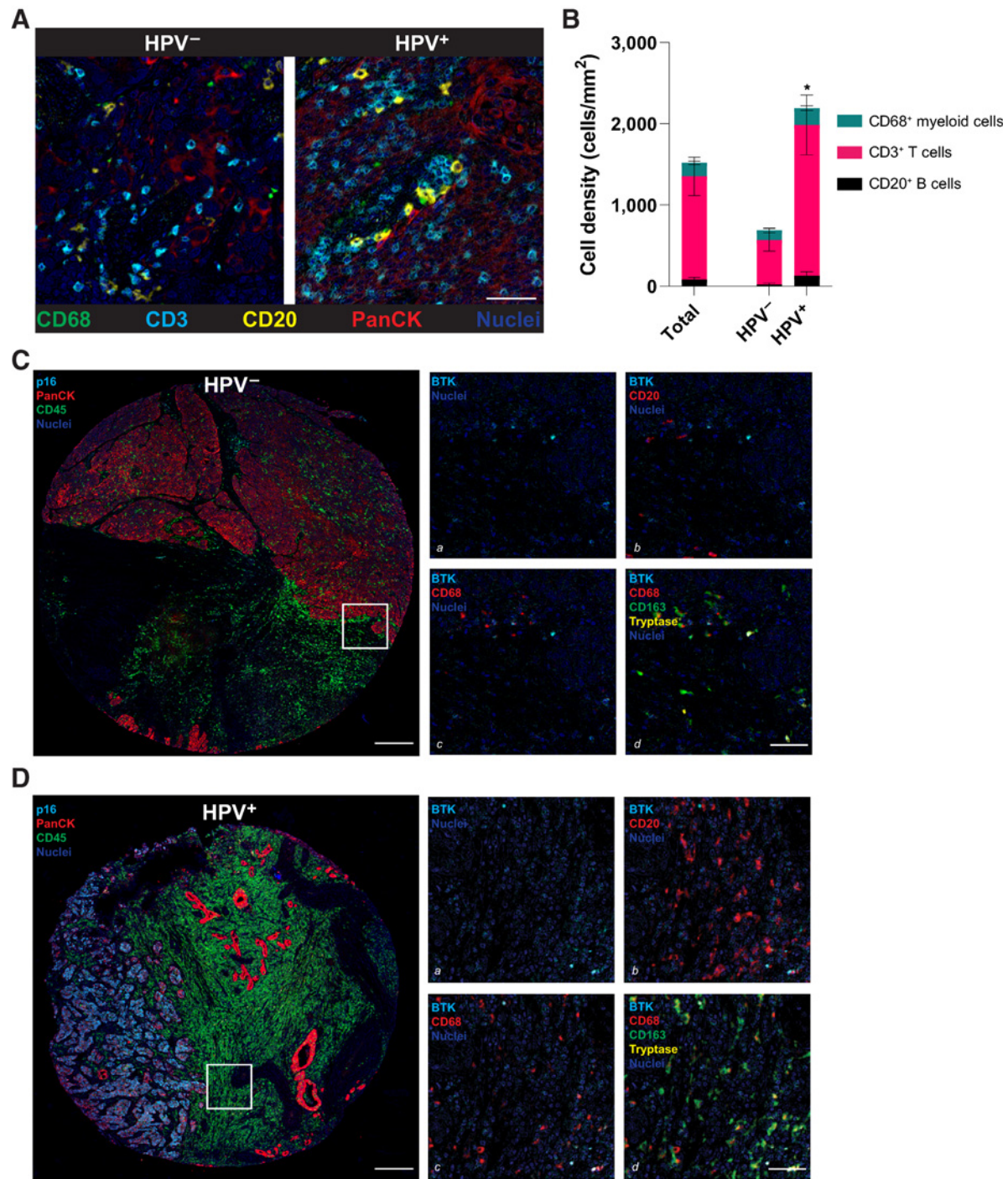
Figure 1.
Immune cell abundance in HPV$^-$ and HPV$^+$ HNSCC tumors. **A,** Pseudocolored images from mIHC staining of representative HPV$^-$ and HPV$^+$ HNSCC tumors, indicating neoplastic (PanCK$^+$) and immune (CD68, CD3, and CD20) cell lineages. **B,** Quantitation of CD68$^+$ myeloid cell (CD45$^+$CD3/CD20/CD56$^-$CD66b$^-$Tryptase$^-$CD68$^+$CSF1R$^+$CD163$^{+/-}$), CD3$^+$ T cell (CD45$^+$CD3$^+$), and CD20$^+$ B cell (CD45$^+$CD3$^-$CD56$^-$CD20$^+$) abundance in all HNSCC samples evaluated (left bar, "total") and stratified by HPV status: HPV$^-$ ($n = 17$) and HPV$^+$ ($n = 21$) HNSCCs. Stacked bars indicate mean $\pm$ SEM. Asterisks, $P < 0.05$ for CD3$^+$ T cell abundance (pink). Pseudocolored images showing BTK immunoreactivity and co-expression with lymphoid and myeloid lineage markers in HPV$^-$ (**C**) and HPV$^+$ (**D**) HNSCC. Low-magnification images at left show representative tissue microarray cores showing location of HPV$^-$ (p16$^-$) and HPV$^+$ (p16$^+$; cyan) neoplastic (PanCK$^+$; red) cells in proximity to immune cell (CD45$^+$; green) infiltrates. Higher magnification regions (boxed area from left panels shown at higher magnifications on right) show BTK positivity (a, cyan) alone, in addition to CD20 (b, red), CD68 (c, red), and together with CD68 (red), CD163 (green), and Tryptase (yellow; d). Co-localization of BTK staining with CD163 and mast cell tryptase staining (d) is evident. BTK, Bruton's tyrosine kinase; HNSCC, head and neck squamous cell carcinoma; HPV, human papillomavirus; PanCK, pan-cytokeratin; SEM, standard error of the mean.

Table 1. Demographics and baseline characteristics.

	Pembrolizumab monotherapy ($n = 39$)[a]	Pembrolizumab plus acalabrutinib ($n = 37$)	Total ($N = 76$)
Age, median (range), y	61.0 (38.0–83.0)	58.0 (45.0–97.0)	60.5 (38.0–97.0)
Sex, male, *n* (%)	34 (87.2)	35 (94.6)	69 (90.8)
Race, *n* (%)			
Asian	2 (5.1)	2 (5.4)	4 (5.3)
Black or African American	0	6 (16.2)	6 (7.9)
White	37 (94.9)	29 (78.4)	66 (86.8)
ECOG PS, *n* (%)			
0	9 (23.1)	9 (24.3)	18 (23.7)
1	30 (76.9)	28 (75.7)	58 (76.3)
Disease stage, *n* (%)			
Stage I[b]	0	1 (2.7)	1 (1.3)
Stage II[c]	0	1 (2.7)	1 (1.3)
Stage III[d]	0	1 (2.7)	1 (1.3)
Stage IVA[e]	13 (33.3)	11 (29.7)	24 (31.6)
Stage IVB[f]	2 (5.1)	1 (2.7)	3 (3.9)
Stage IVC[g]	24 (61.5)	22 (59.5)	46 (60.5)
Number of prior systemic regimens[h], median (range)	2 (1–5)	2 (1–7)	2 (1–7)
Number of prior systemic regimens, *n* (%)			
1	9 (23.1)	8 (21.6)	17 (22.4)
2	14 (35.9)	13 (35.1)	27 (35.5)
≥3	16 (41.0)	16 (43.2)	32 (42.1)

Abbreviations: ECOG PS, Eastern Cooperative Oncology Group performance status; M, metastasis; N, node; T, tumor.
[a]AEs experienced up to crossover date are summarized under pembrolizumab arm.
[b]Defined as T1, N0, M0.
[c]Defined as T2, N0, M0.
[d]Defined as either (i) T3, N0–N2, M0, or (ii) T1/T2, N2, M0.
[e]Defined as either (i) T1–T3, N2, M0; (ii) T4A, N0–N2, M0; (iii) T4, N0–N2, M0; (iv) T4A, N0/N1, M0; or (v) T1–T4A, N2, M0.
[f]Defined as either (i) Any T, N3, M0; (ii) T4B, any N, M0; (iii) T4B, any N, M0; or (iv) any T, N3, M0.
[g]Defined as any T, any N, M1.
[h]Prior definitive or adjuvant therapy.

Table 2. Summary of adverse events.

	Pembrolizumab monotherapy ($n = 39$)	Pembrolizumab plus acalabrutinib ($n = 37$)	Total ($N = 76$)
AEs (all grades)	39 (100)	37 (100)	76 (100)
Grade 3–4	15 (38.5)	24 (64.9)	45 (59.2)
AEs related to pembrolizumab (all grades)	23 (59.0)	11 (29.7)	36 (47.4)
Grade 3–4	3 (7.7)	6 (16.2)	11 (14.5)
AEs related to acalabrutinib (all grades)	0	12 (32.4)	18 (23.7)
Grade 3–4	0	3 (8.1)	5 (6.6)
AEs related to pembrolizumab and acalabrutinib (any grade)	0	19 (51.4)	23 (30.3)
Grade 3–4	0	6 (16.2)	6 (7.9)
SAEs	12 (30.8)	25 (67.6)	45 (59.2)
Related to pembrolizumab	1 (2.6)	3 (8.1)	5 (6.6)
Related to acalabrutinib	0	1 (2.7)	2 (2.6)
Related to pembrolizumab and acalabrutinib	0	3 (8.1)	3 (3.9)
AEs leading to study drug modification	0	2 (5.4)	4 (5.3)
AEs leading to study drug delay	5 (12.8)	17 (45.9)	26 (34.2)
AEs leading to study drug discontinuation	3 (7.7)	7 (18.9)	16 (21.1)
Fatal/grade 5 AEs	1 (2.6)	3 (8.1)	7 (9.2)

Abbreviations: AE, adverse event; SAE, serious adverse event.
[a]Crossover is not the originally randomized group. AEs experienced up to crossover date are summarized for pembrolizumab arm; AEs on or after the crossover date are summarized for the crossover group.

3 patients in the pembrolizumab monotherapy arm (2 receiving crossover treatment at the time of death) and 3 patients in the combination arm. AEs leading to death in the pembrolizumab monotherapy arm were cardio-respiratory arrest, hypoxic-ischemic encephalopathy, and multiple organ dysfunction syndrome ($n = 1$; all reported in the same patient), failure to thrive ($n = 1$, crossover patient), and myocardial infarction ($n = 1$, crossover patient); AEs leading to death in the combination treatment arm were hemorrhage ($n = 1$), respiratory failure ($n = 1$), and sepsis ($n = 1$).

Efficacy

The ORR was 17.9% [95% confidence interval (CI), 7.5%–33.5%] in the pembrolizumab monotherapy arm and 13.5% (95% CI, 4.5%–28.8%) in the pembrolizumab plus acalabrutinib arm (**Fig. 2A–C**). The DCR was 48.7% (95% CI, 32.4%–65.2%) in the pembrolizumab monotherapy arm and 54.1% (95% CI, 36.9%–70.5%) in the pembrolizumab plus acalabrutinib arm. For the 14 patients who crossed over to the combination treatment arm, ORR was 0% (95% CI, 0.0%–23.2%) and DCR was 21.4% (95% CI, 4.7%–50.8%). The median DOR
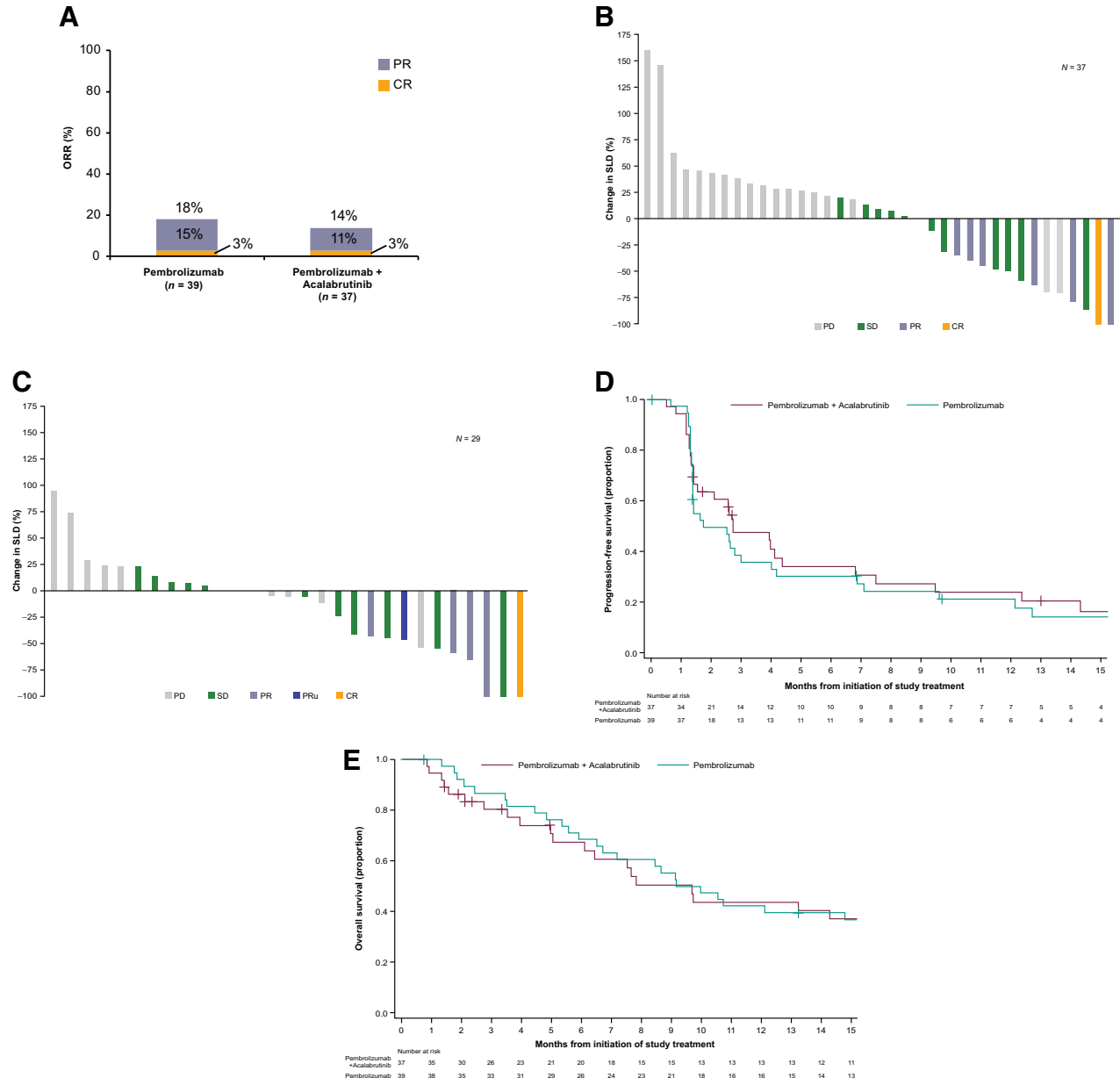
Figure 2.
ORR rate (**A**), best reduction from baseline in the SLD with pembrolizumab monotherapy (**B**) and acalabrutinib + pembrolizumab combination therapy (**C**), progression-free survival (**D**), and overall survival (**E**) by the treatment group. CR, complete response; ORR, overall response rate; PR, partial response; SLD, sum of longest diameters.

among patients with best responses of partial response or better in the monotherapy ($n = 7$) and combination therapy ($n = 6$) arms were 8.4 months (95% CI, 4.1 months–not reached) and not reached (95% CI, 2.4 months–not reached), respectively.

At the time of database lock, 80% of patients in the pembrolizumab monotherapy arm and 73% of patients in the pembrolizumab plus acalabrutinib arm had either progressed due to disease or died. The median PFS was 1.7 months (95% CI, 1.4–4.0 months) in the monotherapy arm and 2.7 months (95% CI, 1.4–6.8 months) in the combination arm (**Fig. 2D**), and the median OS was 9.6 months (95% CI, 6.5–16.1 months) and 9.7 months (95% CI, 5.0–17.4 months), respectively (**Fig. 2E**).

PKs

PK parameters for acalabrutinib were not significantly different with the addition of pembrolizumab (week 1 vs. 7) for $AUC_{0\text{-last}}$ [geometric mean (CV%): 811 (58.2%; $n = 4$) vs. 736 (16.7%; $n = 5$), respectively], C_{max} [geometric mean (CV%): 691 (93.4%; $n = 4$) vs. 598 (34.6%; $n = 6$), or T_{max} [median (range): 0.73 (0.48–2.1; $n = 4$) vs. 0.98 (0.47–1.6; $n = 6$)].

PD-L1 status

PD-L1 status was available in 28 of 39 patients in the pembrolizumab monotherapy arm and 21 of 37 patients in the pembrolizumab plus acalabrutinib arm. Among these patients, 20 were PD-L1 positive (71%), 1 was negative (4%), and 7 samples were not evaluable (25%) in the monotherapy arm, and 12 were PD-L1 positive (57%), 5 were negative (24%), and 4 samples were not evaluable (19%) in the combination treatment arm.

Longitudinal changes in immune contexture pre- and post-treatment

Phenotyping of leukocyte subsets within the lymphoid and myeloid lineages was performed in biopsy specimens from 9 patients (monotherapy, $n = 5$; combination therapy, $n = 4$; Supplementary Table S2). Among the 9 patients with available samples, best treatment response was stable disease in 1 patient who received combination treatment and disease progression in all other patients. In 7 of these patients (monotherapy, $n = 5$; combination therapy, $n = 2$) data from both baseline and on-treatment (day 43) samples were available; in the other 2 patients (both from the combination arm), only data from baseline samples were available. Because the combination arm only contained 2 patients with matched baseline and on-treatment samples, statistical analyses were not possible for this group. Treatment with pembrolizumab monotherapy was associated with a trend toward increased $CD45^+$ leukocyte density from baseline at day 43 ($P = 0.0625$); a similar trend was seen in combination-treated patients (**Fig. 3A**). In both treatment arms, the relative frequencies of other major leukocyte subsets and the overall immune cell composition were generally similar at baseline compared with after treatment, regardless of HPV status as indicated by epithelial p16 positivity (**Fig. 3B** and **C**). A trend toward an increase in Th1:Th2 ratio in Th cells was observed with both monotherapy (3 of 5 patients) and combination treatment (2 of 2 patients) but did not reach statistical significance (**Fig. 4A**). Of note, increases in Th1:Th2 and Th1:Treg ratios in Th cells were observed in both patients from the combination therapy arm who had paired pre- and post-treatment samples (**Fig. 4A** and **B**). Increases from baseline in $CD8^+$ T cell abundance and $CD8^+$ T cell:$CD68^+$ myelomonocytic cell ratio were observed in 4 and 3 of the 5 monotherapy patients with paired samples, respectively (Supplementary Figs. S3A and S4C, respectively); an increase from baseline also was noted

in 1 of 2 patients receiving combination treatment. However, neither the increased abundance of $CD8^+$ T cells nor the increased ratio of $CD8^+$ T cells correlated with a shift toward increased density of mature (DC-LAMP$^+$) DCs (**Fig. 4D**). Although granulocyte presence was modestly reduced in all patients after 43 days on treatment (Supplementary Fig. S3B), no consistent differences in $CD163^+$ expression within the myeloid compartment (Supplementary Fig. S3C) or ICOS$^+$ Th cells (Supplementary Fig. S3D) with treatment versus baseline were observed. Among $CD45^+CD3^+CD8^+$ cells, the proportion of Tbet$^+$EOMES$^+$ cells increased from baseline with treatment in 4 of the 7 patients with paired samples (Supplementary Fig. S4), potentially indicative of a role in late effector T cell accumulation in these tumors.

Discussion

In this proof-of-principle study, no increase in ORR or PFS was demonstrated with the addition of the BTK inhibitor acalabrutinib to the PD-1 inhibitor pembrolizumab in patients with recurrent or metastatic HNSCC, whereas the incidences of grade 3–4 AEs and serious AEs were higher with combination treatment. The study was terminated by the sponsor due to the lack of clinical benefit observed with combination treatment compared with pembrolizumab monotherapy. Despite the lack of clinical efficacy, TiME changes were observed in both the pembrolizumab monotherapy and combination arms, including a trend toward increased $CD45^+$ leukocyte abundance and potentially affected $CD8^+$ T cell responses/phenotype. Although limited by the small sample size, these changes may indicate that acalabrutinib could potentiate T cell activation in combination with PD-1 blockade if toxicities could be mitigated and drugs were appropriately sequenced for delivery.

At the time the current study was initiated (patient enrollment began in 2015), little was known about the risk of infection with acalabrutinib (17); thus, patients were not administered antibiotics prophylactically. The incidences of infection events in the current study were high, most notably in the pembrolizumab plus acalabrutinib combination therapy arm, in which 76% of patients had infection AEs of any grade compared with 39% in the pembrolizumab monotherapy arm. Of note, these incidences are for the grouped term infection, comprising all AEs falling under the Infections and Infestations system organ class. Although a definitive cause for the elevated infection incidence is not known, several mechanisms could potentially contribute to an increase in infections with BTK inhibition, including disruption of antiviral response regulation (18), disruption of macrophage-mediated phagocytosis of fungal pathogens (19), and impairment of macrophage-mediated processes needed to control bacterial infections (20). Notably, these side effects have not been observed in trials examining CSF1/CSF1R antagonists directly targeting macrophages (21).

An increase in the incidence of elevated transaminases was also observed with combination treatment in the current study; no patients in the pembrolizumab monotherapy group versus 11% of patients in the combination treatment group experienced events. Immune-mediated hepatitis is a known risk for pembrolizumab, so elevated transaminases were not unexpected. In addition, in a comprehensive meta-analysis of randomized immunotherapy trials, patients treated with immune checkpoint inhibitors have been demonstrated to have a significantly higher risk of aspartate aminotransferase elevation (22). This is an expected effect of immune checkpoint inhibitors due to the stimulation of autoreactive T cells, leading to autoimmune-related toxicities, including liver toxicity (23).
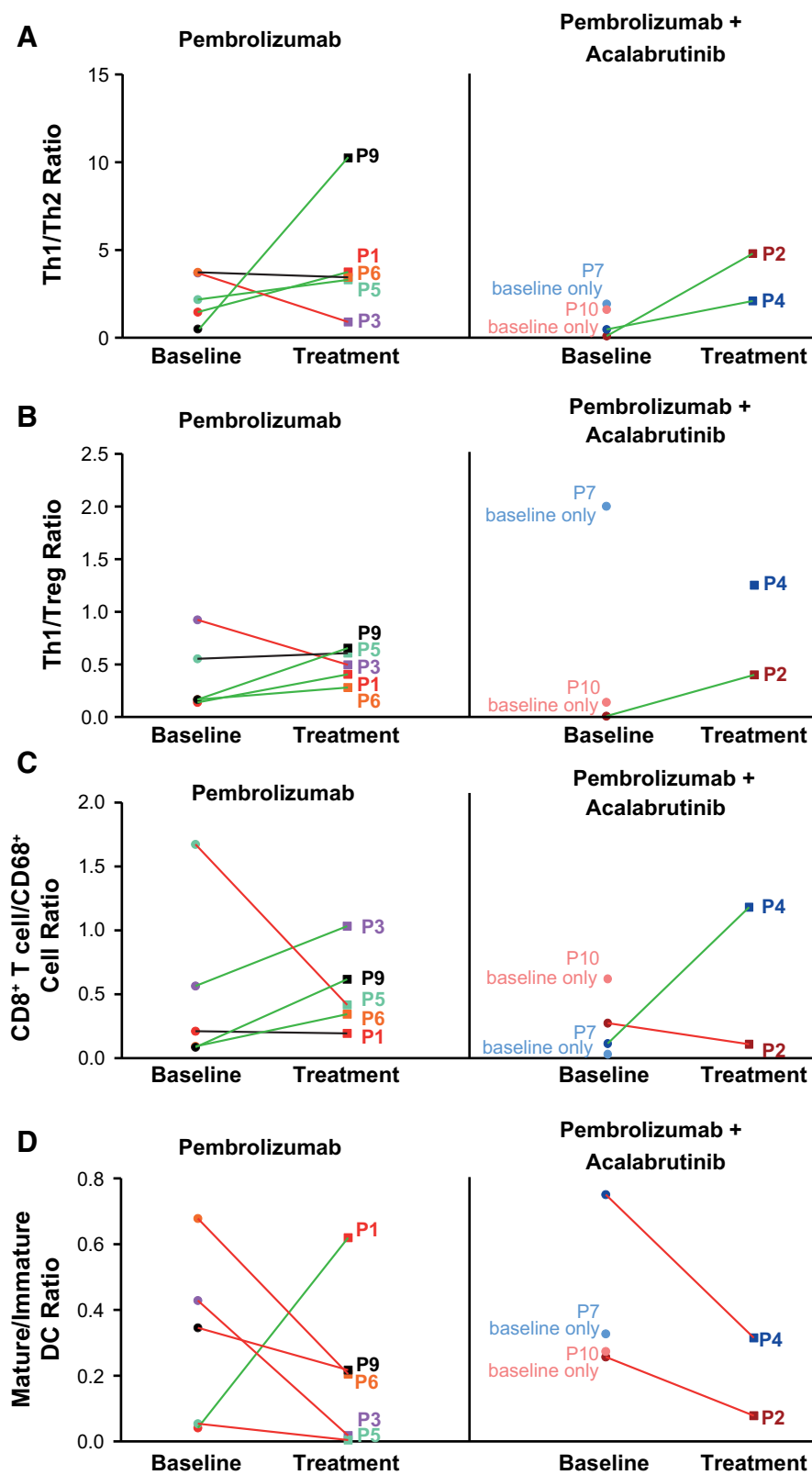
Figure 3.
Leukocyte infiltration at baseline and after 43 days on treatment. **A,** The percentage of total nucleated cells that were CD45$^+$ (total leukocytes) are shown for each patient at baseline and after 43 days of treatment (Rx). Green lines pairing baseline and Rx samples reflect a >10% increase in ratio after treatment compared with baseline. Leukocyte lineage subtypes are shown as the percentages of total CD45$^+$ cells per patient at baseline (**B**) and after 43 days of treatment (**C**). Pembrolizumab monotherapy, $n = 5$; pembrolizumab plus acalabrutinib combination therapy, $n = 4$ at baseline and $n = 2$ with treatment at day 43. Colors delineate cell types as indicated in the legend (right of **B** and **C**). In **B** and **C**, human papillomavirus (HPV) status was evaluated by p16-positivity via a multiplex immunohistochemical platform, and used as a molecular correlate for HPV status, where results are denoted as "+" and "−" for HPV-positive and HPV-negative, respectively.
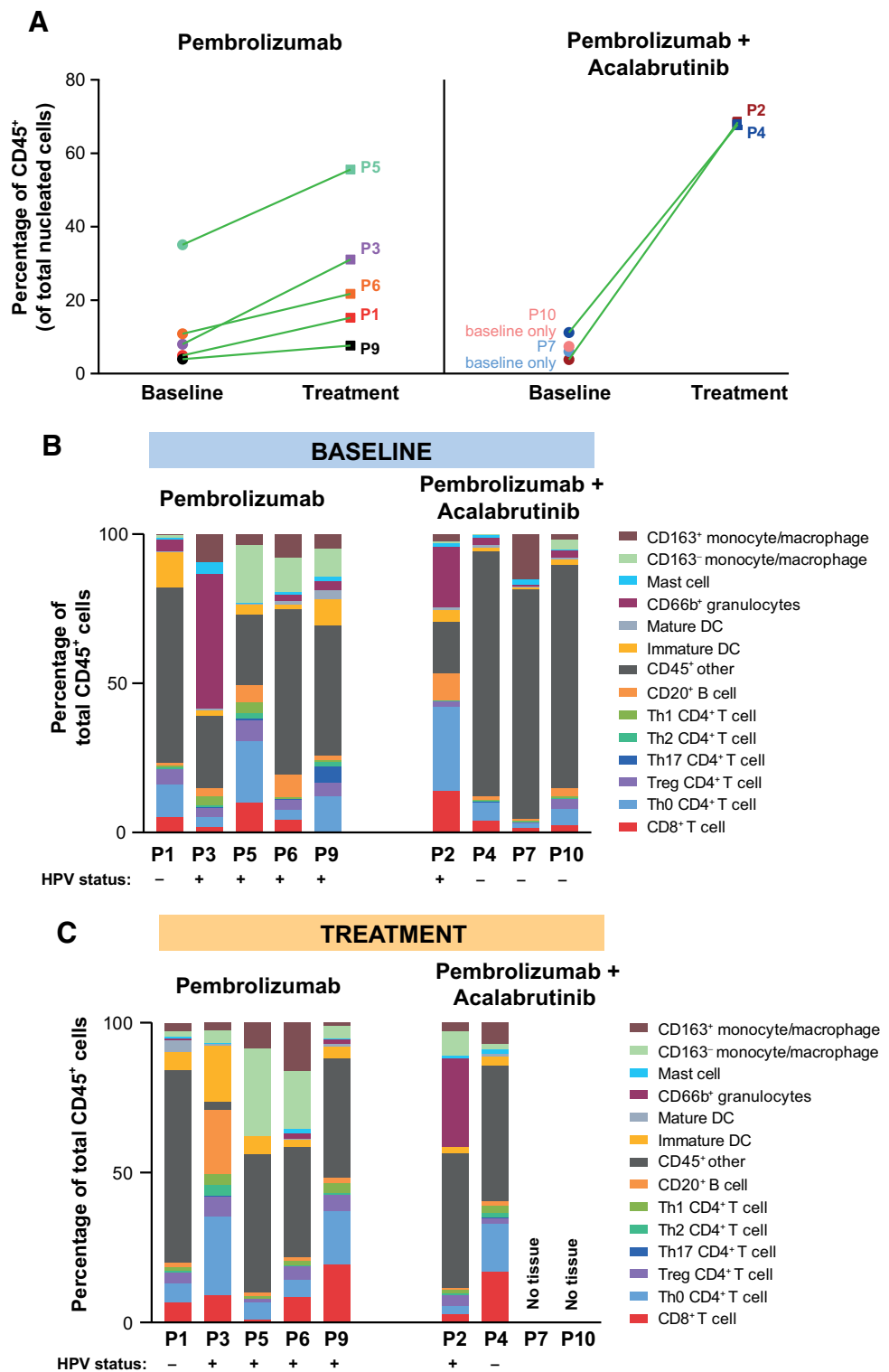
Preclinical studies in murine models of insulinoma and PDAC identified BTK as a significant regulator of myeloid cell functionality and myeloid-mediated T cell suppression (10–12). The immune contexture analyses in the current study demonstrated few BTK$^+$ B cells in HNSCCs independent of HPV status, but substantial BTK expression in CD68$^+$ myelomonocytic cells within HNSCC tumors, potentially, indicating a functional role for BTK in regulating myeloid-mediated T cell suppression in HNSCC. Although limited clinical benefits were observed in this study, several subtle microenvironmental changes with combination treatment were noted. A trend toward

Figure 4.
TiME at baseline and after treatment. Ratios of (**A**) Th1 (Tbet$^+$) to Th2 (GATA-3$^+$) CD4$^+$ T cells, (**B**) Th1 (Tbet$^+$) to Treg (FoxP3$^+$) CD4$^+$ T cells, (**C**) CD8$^+$ T cells to CD68$^+$ monocytes/macrophages, and (**D**) mature (DC-LAMP$^+$) to immature (DC-LAMP$^-$) DCs are shown for each patient at baseline and after 43 days of treatment (Rx). Pembrolizumab monotherapy, $n = 5$; pembrolizumab plus acalabrutinib combination therapy, $n = 4$ at baseline and $n = 2$ at day 43. Green lines pairing baseline and Rx samples reflect a >10% increase after treatment compared with baseline, red lines indicate a >10% decrease after treatment compared with baseline, and black lines indicate a change of <10% after treatment compared with baseline. DC, dendritic cells; Th, T helper; TiME, tumor-immune microenvironment; Treg, regulatory T cells.

increased CD45^{+} leukocyte abundance was observed after treatment with pembrolizumab, which was modestly augmented by addition of acalabrutinib, indicating a potential additive effect with combination therapy. In addition, a trend toward an increased abundance of Th1: Th2, Th1:Tregs, and CD8^{+} T cell:CD68^{+} cell ratios with pembrolizumab, alone or in combination with acalabrutinib treatment, was observed. Furthermore, an increased abundance of CD8^{+} T cells was observed in 4 of 5 pembrolizumab-treated patients and 1 of 2 combination-treated patients (Supplementary Fig. S3A), and the proportion of CD8^{+} T cells expressing Tbet and EOMES, defined as effector memory cells, was increased in 3 of 5 pembrolizumab-treated patients and 1 of 2 combination-treated patients (Supplementary Fig. S4), indicating a potential impact on CD8^{+} T cell responses. However, definitive effects of combination treatment versus pembrolizumab alone are difficult to discern and meaningful conclusions cannot be drawn given the low number of samples in the current study. However, these results are fairly consistent with preclinical murine models of pancreatic cancer in which BTK inhibition, when sequenced before chemotherapy in a 1-week run-in, resulted in increased numbers of tumor-associated CD8^{+} T cells and suppressed tumor growth evidencing the utility of BTK inhibition in remodeling the TiME (11). Similar boosts in CD8^{+} T cell response have been observed in clinical studies with the BTK inhibitor ibrutinib (24); however, the subtle enhancement in effector memory CD8^{+} T cells in the current study did not correlate with a shift toward increased density of mature DCs, unlike the preclinical models (11). The decrease in mature DC density following pembrolizumab monotherapy and pembrolizumab plus acalabrutinib combination treatment could reflect the need for repriming of T cells by antigen-presenting cells, as was demonstrated in the murine model with concurrent cytotoxic therapy following the BTK inhibitor monotherapy run-in (11).

Data from mouse models indicate that chemotherapy can accentuate T cell responses. In a mouse model of ovarian cancer, paclitaxel treatment combined with PD-L1 blockade led to significantly elevated levels of T cell activation/immune activation following antigen presentation versus levels seen in non-treated cells (25). Chemotherapeutic agents have also been demonstrated to augment T cell response by increasing DC function and upregulating HLA class I expression to enhance T cell recognition of tumor cells *in vitro* (26). These data have led the way to designing trials using chemotherapeutic agents in combination with immune checkpoint inhibitor targeted therapies. The current trial was designed before chemotherapy and immune checkpoint combination trials were initiated. However, although clinical efficacy might have been improved with the addition of chemotherapy to the combination, increased toxicity would have been expected in the absence of appropriate sequencing. Additional limitations of this study include the small sample size, both in terms of the overall number of patients and of the number of baseline and post-treatment paired biopsy samples available for assessment of the effects of combination therapy on the tumor microenvironment.

Results of this study indicated that there is no clinical benefit from adding acalabrutinib to pembrolizumab in the treatment of recurrent or metastatic HNSCC. The immune subset analysis data suggest that there may be additive effects of this combination therapy. Specifically, acalabrutinib could enhance the immune response with pembrolizumab treatment by reprogramming the myeloid compartment, relieving the suppression of CD8^{+} T cells, and increasing memory response, but certainly additional preclinical modeling is needed to elucidate appropriate sequencing and combination strategies. The sample sizes were too small to draw conclusions, and additional research with larger sample sizes would be needed to comprehensively assess the immune-

related effects of pembrolizumab and acalabrutinib combination treatment on the tumor microenvironment.

References

1. US National Library of Medicine. Head and neck squamous cell carcinoma. Genetics Home Reference 2020. [cited 2021 Oct 4]. Available from: https://ghr.nlm.nih.gov/condition/head-and-neck-squamous-cell-carcinoma#statistics.
2. Monnerat C, Faivre S, Temam S, Bourhis J, Raymond E. End points for new agents in induction chemotherapy for locally advanced head and neck cancers. Ann Oncol 2002;13:995–1006.
3. Vermorken JB, Specenier P. Optimal treatment for recurrent/metastatic head and neck cancer. Ann Oncol 2010;21:vii252–61.
4. Canning M, Guo G, Yu M, Myint C, Groves MW, Byrd JK, et al. Heterogeneity of the head and neck squamous cell carcinoma immune landscape and its impact on immunotherapy. Frontiers Cell Develop Biol 2019;7:52.
5. Ang KK, Harris J, Wheeler R, Weber R, Rosenthal DI, Nguyen-Tân PF, et al. Human papillomavirus and survival of patients with oropharyngeal cancer. N Engl J Med 2010;363:24–35.
6. Fakhry C, Westra WH, Li S, Cmelak A, Ridge JA, Pinto H, et al. Improved survival of patients with human papillomavirus-positive head and neck squamous cell carcinoma in a prospective clinical trial. J Natl Cancer Inst 2008;100: 261–9.
7. Burtness B, Harrington KJ, Greil R, Soulières D, Tahara M, de Castro G Jr, et al. Pembrolizumab alone or with chemotherapy versus cetuximab with chemotherapy for recurrent or metastatic squamous cell carcinoma of the head and neck (KEYNOTE-048): a randomised, open-label, phase 3 study. Lancet 2019; 394:1915–28.
8. Kok VC. Current understanding of the mechanisms underlying immune evasion from PD-1/PD-L1 immune checkpoint blockade in head and neck cancer. Front Oncol 2020;10:268.
9. Stiff A, Trikha P, Wesolowski R, Kendra K, Hsu V, Uppati S, et al. Myeloid-derived suppressor cells express Bruton's tyrosine kinase and can be depleted in tumor-bearing hosts by ibrutinib treatment. Cancer Res 2016;76:2125–36.
10. Soucek L, Buggy JJ, Kortlever R, Adimoolam S, Monclus HA, Allende MT, et al. Modeling pharmacological inhibition of mast cell degranulation as a therapy for insulinoma. Neoplasia 2011;13:1093–100.
11. Gunderson AJ, Kaneda MM, Tsujikawa T, Nguyen AV, Affara NI, Ruffell B, et al. Bruton tyrosine kinase-dependent immune cell cross-talk drives pancreas cancer. Cancer Discov 2016;6:270–85.
12. Massó-Vallés D, Jauset T, Serrano E, Sodir NM, Pedersen K, Affara NI, et al. Ibrutinib exerts potent antifibrotic and antitumor activities in mouse models of pancreatic adenocarcinoma. Cancer Res 2015;75:1675–81.
13. Liu SC, Wu YC, Huang CM, Hsieh MS, Huang TY, Huang CS, et al. Inhibition of Bruton's tyrosine kinase as a therapeutic strategy for chemoresistant oral squamous cell carcinoma and potential suppression of cancer stemness. Oncogenesis 2021;10:20.
14. Calquence [package insert]. Wilmington, DE: AstraZeneca Pharmaceuticals; 2019.
15. Tsujikawa T, Kumar S, Borkar RN, Azimi V, Thibault G, Chang YH, et al. Quantitative multiplex immunohistochemistry reveals myeloid-inflamed tumor-immune complexity associated with poor prognosis. Cell Rep 2017;19: 203–17.
16. Banik G, Betts CB, Liudahl SM, Sivagnanam S, Kawashima R, Cotechini T, et al. High-dimensional multiplexed immunohistochemical characterization of immune contexture in human cancers. Methods Enzymol 2020;635: 1–20.
17. Atkins S, He F. Chemotherapy and beyond: infections in the era of old and new treatments for hematologic malignancies. Infect Dis Clin North Am 2019;33: 289–309.
18. Lee KG, Xu S, Kang ZH, Huo J, Huang M, Liu D, et al. Bruton's tyrosine kinase phosphorylates Toll-like receptor 3 to initiate antiviral response. Proc Natl Acad Sci U S A 2012;109:5791–6.
19. Strijbis K, Tafesse FG, Fairn GD, Witte MD, Dougan SK, Watson N, et al. Bruton's tyrosine kinase (BTK) and Vav1 contribute to Dectin1-dependent phagocytosis of Candida albicans in macrophages. PLoS Pathog 2013;9: e1003446.
20. Colado A, Genoula M, Cougoule C, Marín Franco JL, Almejún MB, Risnik D, et al. Effect of the BTK inhibitor ibrutinib on macrophage- and $\gamma\delta$ T-cell–mediated response against Mycobacterium tuberculosis. Blood Cancer J 2018;8: 100.
21. Cannarile MA, Weisser M, Jacob W, Jegg AM, Ries CH, Rüttinger D. Colony-stimulating factor 1 receptor (CSF1R) inhibitors in cancer therapy. J Immunother Cancer 2017;5:53.
22. De Velasco G, Je Y, Bossé D, Awad MM, Ott PA, Moreira RB, et al. Comprehensive meta-analysis of key immune-related adverse events from CTLA-4 and PD-1/PD-L1 inhibitors in cancer patients. Cancer Immunol Res 2017;5:312–8.
23. Suzman DL, Pelosof L, Rosenberg A, Avigan MI. Hepatotoxicity of immune checkpoint inhibitors: an evolving picture of risk associated with a vital class of immunotherapy agents. Liver Int 2018;38:976–87.
24. Long M, Beckwith K, Do P, Mundy BL, Gordon A, Lehman AM, et al. Ibrutinib treatment improves T-cell number and function in CLL patients. J Clin Invest 2017;127:3052–64.
25. Peng J, Hamanishi J, Matsumura N, Abiko K, Murat K, Baba T, et al. Chemotherapy induces programmed cell death-ligand 1 overexpression via the nuclear factor-κB to foster an immunosuppressive tumor microenvironment in ovarian cancer. Cancer Res 2015;75:5034–45.
26. Liu WM, Fowler DW, Smith P, Dalgleish AG. Pre-treatment with chemotherapy can enhance the antigenicity and immunogenicity of tumours by promoting adaptive immune responses. Br J Cancer 2010;102:115–23.